Moving deforming mesh modeling of human organ systems

Hamidreza Mortazavy Beni[a,*], Hamed Mortazavi[a], Gunther Paul[b,*], Mohammad Saidul Islam[c]

[a] Department of Biomedical Engineering, Arsanjan Branch, Islamic Azad University, Arsanjan, Iran.

[b] Australian Institute of Tropical Health and Medicine, James Cook University, Mackay, QLD 4741.

[c] School of Mechanical and Mechatronic Engineering, University of Technology Sydney (UTS),

15 Broadway, Ultimo, NSW-2007, Australia.

Abstract

Dynamic modeling of body organs has become an elementary part of modern digital human modeling (DHM), where advanced biomedical models incorporate biomechanical behavior of tissues down to the cell level. While the biomechanical response of organs to impact and trauma has traditionally been considered an important aspect in developing safety related models such as for vehicle crash simulation, organ behavior is now also reflected in models used for medical purposes, such as the simulation of breathing or cardiovascular circulation. All human body cells have in vivo nonlinear viscoelastic properties. Moreover, body tissue is composed of cells wrapped in an extracellular matrix (ECM). Body tissue in vivo nonlinear viscoelastic properties depend on its function in an organ system, which directly affects the tissue viscoelasticity modulus. For advanced perfusion or fluid passage simulation, we propose to represent the nonlinear viscoelastic behavior of the body tissue in a solid boundary condition using the moving deforming mesh (MDM) method. The MDM method considers the viscoelastic perfusion wall during transient fluid flow responding to the pressure pulse from the human organ systems as the lung or heart. Also, changing the volume fraction of the ECM constituents due to aging or diseases like cancer leads to changes in the viscous modulus (loss modulus) and elastic modulus (storage modulus) of organ tissue. Therefore, the MDM method can produce a reliable result that corresponds to reality by considering the precise viscoelastic properties of the fluid passage wall. In this study, we use the MDM method to examine two organ geometries from the respiratory and cardiovascular systems. Although the simulation effort using this method is more time-consuming, the simulation outcomes are expected to be in better accordance with the real organs when compared to simulation results using the computational fluid dynamic (CFD) method, where perfusion wall behavior is considered to be rigid. In this regard, accurate computational

[*] Corresponding author.
E-mail address: gunther.paul@jcu.edu.au (Gunther Paul).
E-mail address: HRM.Beni@iau.ac.ir & HRM.Beni@gmail.com (Hamidreza Mortazavy Beni).

modeling leads to pre-visualizing in surgical planning to define the best favorable reformative techniques to determine the most probable patient condition consequences.

Keywords Respiratory, Cardiovascular, In silico modeling, Viscoelasticity, Cancer.

Introduction

Throughout modern medical history, study of the functions of human body organs has always been a focus of research. In modern societies however ethical restrictions impose significant limitations on the study of organs to be examined in vivo, whereas most organ functions cannot be accessed in vitro. Mathematical modeling methods based on the use of powerful computers and software inform the modern and state-of-the-art way of in vitro simulation to avoid any experimental restrictions. In the human body, functions of the respiratory system and the circulatory system are closely related. Humans in average breathe about 6 liters of air per minute, which coincides with the volume of blood the heart pumps each minute. In this paper, selected functions of these two important organs of the body are modelled and investigated using the moving deforming mesh (MDM) method, with a restriction to the upper respiratory system and the circulatory system in the aorta.

Respiratory System

The nose, nasal cavity, and sinuses form the intricate geometry of the upper respiratory tract. The nose performs important physiological functions, including thermal management (heat, humidity), air filtration, and odor inhalation. The nose also separates breathable air from pollution and toxic particles that may enter its tract. More advanced aspects of toxicology, particle dispersion, the effect of drugs, filtration of airborne particles from the respiratory air, and planning for surgery have been discussed after the study of dynamic characteristics of airflow in the nasal passages. In the CFD method though, a rigid airway wall is assumed which contradicts the actual viscoelastic behavior of the airway. Therefore, this study aims to expand our understanding how airflow behaves in the upper respiratory system by using the moving deforming mesh (MDM) method which considers a viscoelastic behavior of the airway.

Circulatory System

Accumulation of fatty deposits in blood vessels causes narrowing of arteries and impaired blood flow. This condition, called atherosclerosis, causes many problems in the circulatory system. One of the vessels in which the onset of this disease is critical is the aortic arch, which eventually leads to the risk of rupture of the vessel wall by creating an aneurysm. Most previous numerical studies on atherosclerosis are based on the CFD method, in which the arterial wall is assumed to be rigid [1].

Tissue behavior however is viscoelastic, and the rate of change in duct diameter in systole and diastole is high. In this study, the behavior of the aortic arch is examined using the MDM method.

Methods

Geometry of models

The models are based on CT scan images which represent a wide range of different tissues. By adjusting a grey value threshold, the desired organ is extracted. Under expert supervision, the boundary between fluid and wall is determined and considered in the CT image segmentation. The borders are connected to create a continuous and smooth surface and species volume. This study is based on computerized radiography of the head, neck, and chest of a 70-year-old smoker with a height of 170 cm, weighing 75 kg with a tumor in the upper respiratory tract in the larynx [2]. Fig. 1a shows the respiratory system studied in this study. The model includes the nasal cavity, nasopharynx, oropharynx, larynx, and trachea. Fig. 1b shows the aortic system studied in this study. This model includes the aortic arch with the descending aorta (DA) , Left Common Carotid artery (LCC), Left Subclavian artery (LS), Brachiocephalic Trunk (BT), and the Ascending Aorta (AA).

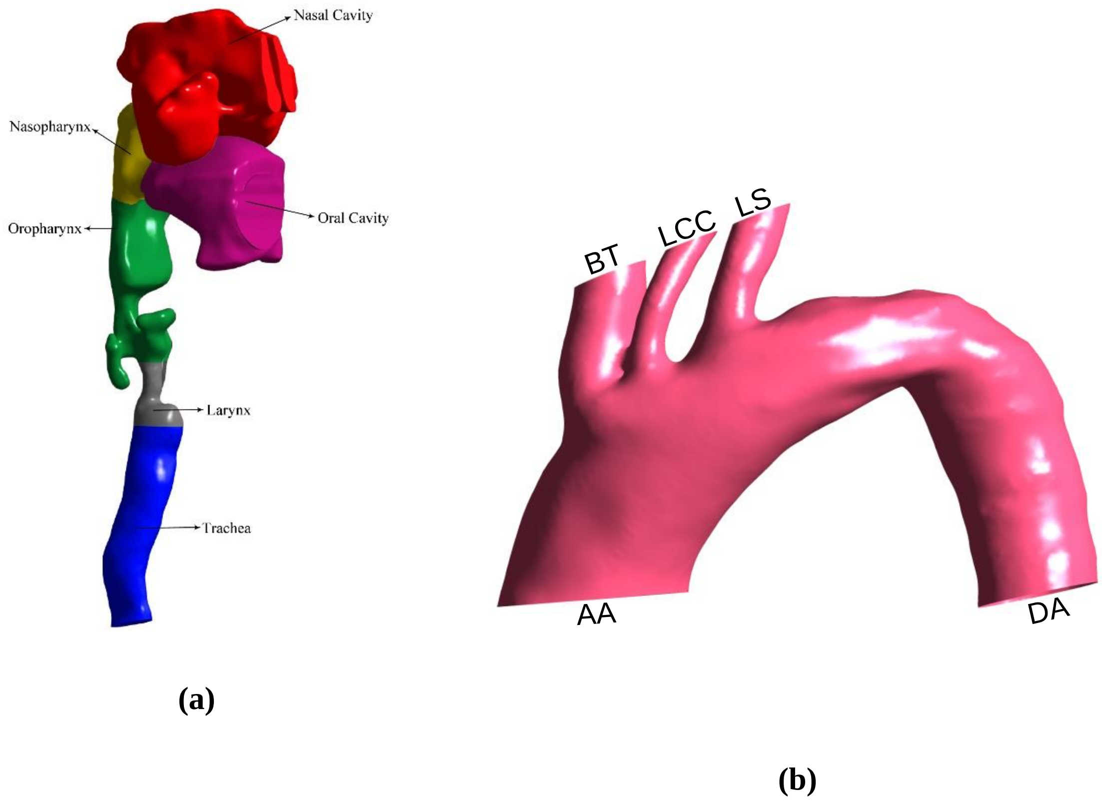

Figure 1. The geometry of the upper respiratory system and the aortic arch in the present study. (**a**) Upper respiratory system. (**b**) Aortic arch.

In a fluid domain, solving nonlinear equations of continuity and momentum is necessary. In these equations, velocity and pressure are coupled. Also, due to the pulsed flow in the respiratory system and blood circulation, the analysis of changes at the interface between the fluid passage and the solid wall is dynamically transient. Governing equations were presented in previous studies and are not mentioned again for the sake of brevity [3, 4].

Respiratory system

Due to the low air velocity, incompressible and laminar flow is considered at resting status. The physical properties of air are selected at 37 °C. Other physical properties such as Young's modulus of 100.64 kPa and the Poisson's ratio of 0.33 have been selected for solid walls based on a previous study [5].

Circulatory system

In this case, blood is considered an incompressible and turbulent fluid. An important characteristic of turbulent flow is that it is not silent. The heart sounds heard with a stethoscope are caused mostly by turbulent flow. Turbulent flow occurs at the opening and closing of heart valves. Thus the flow is turbulent during part of the systole. The physical properties of blood at 37 °C are considered. According to the previous study, physical properties such as Young's modulus of 0.88 MPa and the Poisson's ratio of 0.17 have been selected for solid walls [6].

Boundary Conditions

Creating any physical or computational model of flow requires recognizing and defining the boundaries of the fluid passage. In practice, the boundaries of the biomechanical fluid passage and the flow rate of the fluid change with time. Also, the geometric structure of the fluid passage alone has a great influence on the dynamics of the fluid inside it. In the present work, modeling was done in the individual's resting condition. Two basic boundary conditions are used at the boundary of fluid and solid domains. Firstly, there is a non-slip condition along the wall, where the values of the fluid velocity components are zero. Secondly, the MDM boundary condition between fluid and solid is assumed. The output results of the simulation are studied after several cycles of repeated fluid flow in a transient condition to ensure that the responses are stable.

Respiratory system

The exhale airflow rate is applied for normal inhalation at rest. Therefore, the amplitude of 6 l/min is set at the inlet of the trachea. Inhalation and exhalation are performed in a 4 seconds period. Then the inlet velocity equation is defined by the relation of:

$$V = 6\sin\frac{\pi}{2}t \tag{1}$$

The pressure conditions at the nostrils outlet are set to 101,325 Pa (1 atm). In this model, a closed mouth is assumed. For the solid domain, the fixed support boundary condition is applied for the model inputs in the trachea and the model outputs in the nose. Additionally, after the transient flow conditions have stabilized, cigarette smoke particles with a diameter of 1 μm and a density of 1200 $^{kg}/_{m^3}$ are injected into the model to observe the pattern of particle deposition during exhalation.

<u>Circulatory system</u>

The cardiac cycle includes systole and diastole and lasts for about 0.8 seconds per period. In the current model, the boundary conditions are adjusted for the inlets and outlets of the aorta in accordance with Fig. 2 [7]. These conditions are applied in the simulation with the help of a user-defined function (UDF) definition. For the solid domain, the fixed support boundary condition is applied for model input in AA and model outputs in BT, LCC, LS, and DA. In addition, after the transient flow conditions stabilize, fat particles with a diameter of one micron and a density of 900 $^{kg}/_{m^3}$ are injected into the model to observe the pattern of particle deposition in the aortic wall.

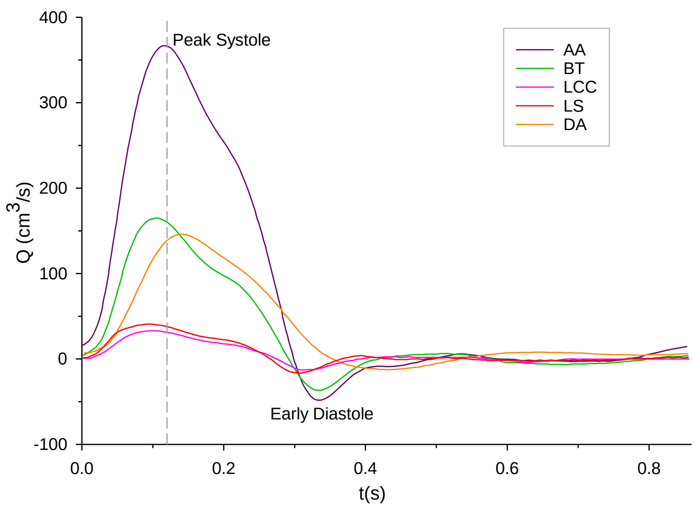

Figure 2. Boundary condition definition in the inlet and outlets of the aortic arch.

Numerical Solution

Fluid and solid fields are divided into computational elements to solve the governing equations. The very fine mesh for the solid domain is selected, and different mesh numbers for the fluid domain are considered to ensure the accuracy of the results of the produced mesh. The fluid grid generation is chosen so finely that the difference between the results obtained during the previous cycle can be ignored. The mesh created in this model contains tetrahedral elements for the respiratory and aortic systems, 3,502,459 and 1,312,338 respectively, after examining a grid independency analysis. Nonlinear analysis is necessary for large deformations. As a solver for the Lagrangian formulation of the solid model and the Arbitrary Lagrangian-Eulerian (ALE) formulation of the fluid model Ansys 2021 R1 software (ANSYS, Inc., Canonsburg, PA, USA) is used. The $k - \varepsilon$ turbulence model is used to solve the turbulent flow in the aorta. The number of iterations and the convergence criterion for both solid and fluid models are 100 and 0.001 in a 0.001 s time step, respectively. Eliminating the effect of initial conditions in periodic nonlinear problems is important. Five consecutive cycles are repeated to achieve a stable cycle, and the results presented are related to the fifth cycle.

Results

While the MDM method provides simulated analytic results for the two studies of the vital organs, a comparison between fluid velocity profiles in experiment and simulation is required to validate the modeling. Ball et al. [8] have used hot-wire anemometry to obtain experimental analytic results on the respiratory system, producing similar results to this study. Tse et al. [9] have reported time-averaged wall shear stress (WSS) results for six different human models of aortic geometry in a different CFD study, with less than 5% deviation to results of this study.

Respiratory System

Fig. 3a and Fig. 3b show the exhalation streamline and velocity vector pattern for the respiratory model at peak exhalation at 6 l/min, respectively. At the site of the larynx, with airway stenosis due to the presence of a tumor, a maximum velocity of 2.6 m/s is observed. Airflow recirculation in the oropharyngeal region is considerable. Fig. 3c shows the pressure contour in exhalation for the respiratory model. The trachea bears the most pressure, and its value is uniformly equal to 3.5 Pa along the trachea. Fig. 3d shows the WSS contour in exhalation. The larynx and oropharynx tolerate most WSS at 0.36 Pa. Fig. 3e and Fig. 3f show the stress and strain at the time of exhalation, respectively. The highest stress and strain are observed in the trachea, at 23 Pa and 2.3×10^{-4}, respectively. Fig. 3g shows the displacement contour during exhalation. The oropharyngeal region tolerates most displacement, equating to 0.005 mm. Fig. 3h shows the deposition contour in exhalation. The larynx and oropharynx are the most affected areas. The percentage of total deposition in the model is 8.3%.

Circulatory System

Fig. 3a and Fig. 3b show the streamline and velocity vector pattern in the aortic arch model at systolic peak, respectively. The highest blood velocity in the aortic arch is 1.7 m/s. Also, the maximum pressure is equal to 11.7 kPa. Fig. 4c shows the aortic model's Y^+ contour at the peak systole. The maximum Y^+ reaches 7.4. This indicates that a high quality grid was generated and that the right solution method was chosen for the turbulent aortic blood flow. Fig. 4d shows the WSS contour at peak systole. The highest WSS is located at the entrance, the branches root and the abdominal aorta; its value reaches 55.9 Pa. Fig. 4e and Fig. 4f show the stress and strain

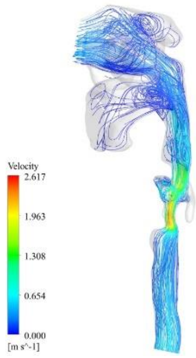

(a)

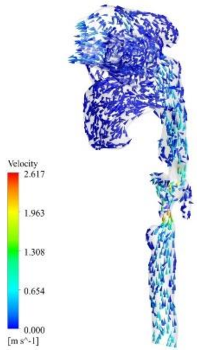

(b)

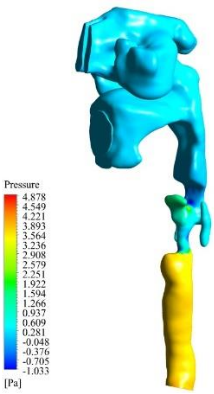

(c)

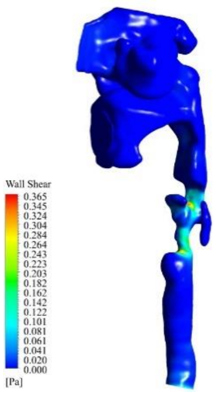

(d)

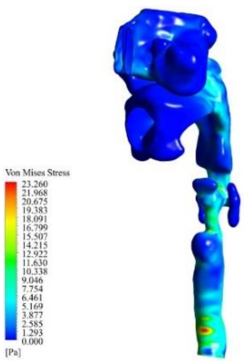

(e)

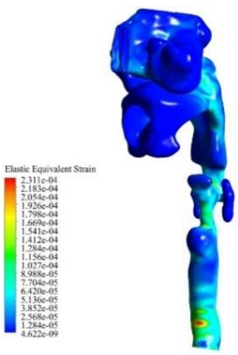

(f)

(g) **(h)**

Figure 3. The contour of streamlines, velocity vector, pressure, WSS, stress, strain, deformation, and deposition pattern in the upper airway for a rest condition of peak exhalation at 6 l/min. (**a**) Streamlines. (**b**) Velocity vector. (**c**) Pressure. (**d**) WSS. (**e**) Von Mises stress. (**f**) Elastic equivalent strain. (**g**) Total mesh displacement. (**h**) Deposition pattern.

at peak systole, respectively. The highest stress and strain are observed at the supra-aortic branches. Fig. 4g shows the displacement contour at peak systole. The maximum displacement is found in the descending aorta zone reaching 0.08 mm. Fig. 4h shows the deposition contour at peak systole. Most deposition occurs at the ascending aorta and the location of the branches root and the descending aorta. The percentage of total deposition in the model is 8.2%. Notably, 84.8% of fat particles escape to the abdominal aorta.

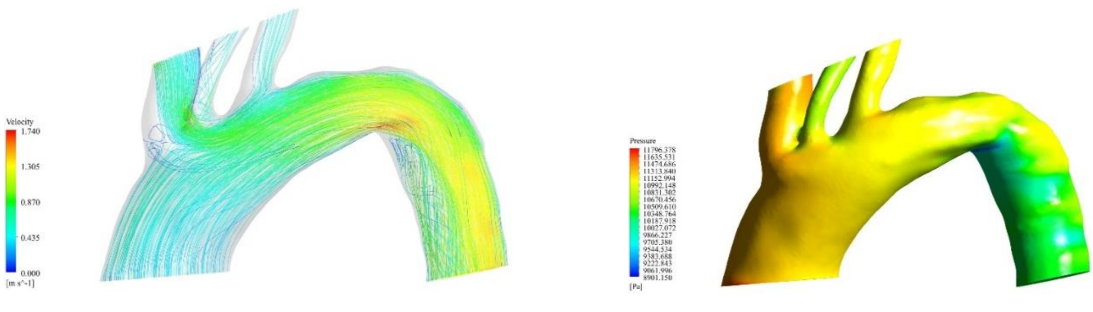

(a) **(b)**

(c)

(d)

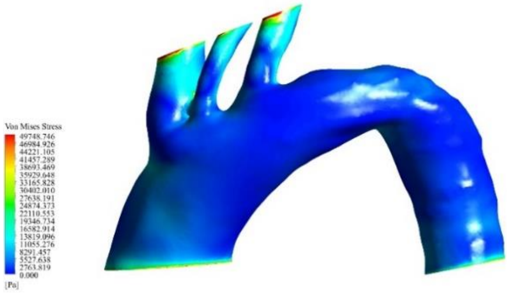

(e)

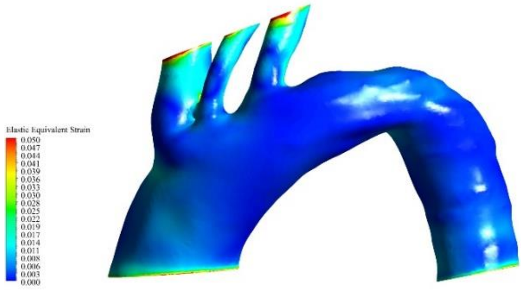

(f)

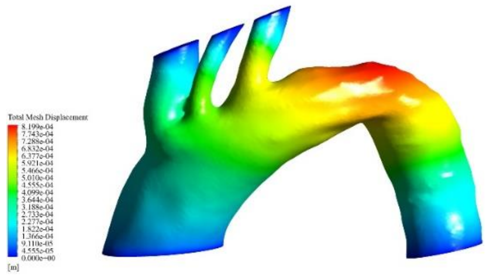

(g)

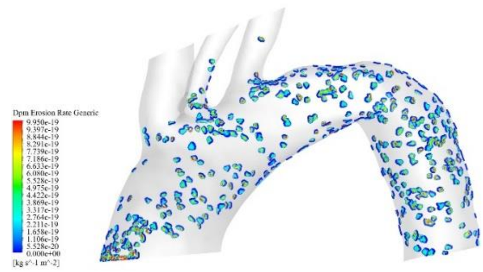

(h)

Figure 4. The contour of streamlines, pressure, Y^+, WSS, stress, strain, deformation, and deposition pattern in the aortic arch for a rest condition of systolic peak. (**a**) Streamlines. (**b**) Pressure. (**c**) Y^+ variation in the geometry domain. (**d**) WSS. (**e**) Von Mises stress. (**f**) Elastic equivalent strain. (**g**) Total mesh displacement. (**h**) Deposition pattern.

Discussion and Conclusion

With the help of accurate numerical methods, the conditions are provided for examination of the human body in a way that in vitro results can accurately predict in vivo processes in the body [10, 11]. The present study simulated two essential and related body organs, namely the circulatory system and the respiratory system, using the MDM method at rest condition. In the upper airway, the larynx and oropharynx tolerate most WSS. On the other hand, those are the most affected areas by cigarette smoke particles. In the circulatory system, the abdominal aorta is a high-risk zone for fat particles to settle. Indeed most fat particles accumulate in the abdominal aorta, which may be due to the lower speed of blood flow and longer path in the abdominal aorta. Also noteworthy in both the respiratory and the aorta models is that in places of geometry with the maximum WSS, particle deposition is highest. In other words, the deposition pattern of particles is directly related to the WSS index.

Digital human modeling of fluid flow can be essential in understanding and treating disease. It is necessary to conduct further studies on pulmonary blood flow and hemodynamic behavior of patient blood flow to reduce the risk of invasive vascular surgery. The present study used CT images to determine boundary conditions of the aortic and respiratory systems. Models showed that the junctions of bifurcation have a higher risk of particle deposition. The values of instantaneous hemodynamic parameters in the rigid wall state are far from the elastic wall state. Using viscolelastic wall modeling improved results vs. CFD-based rigid wall models. An important result of the current model-based simulation is that particle deposition was highest in both the respiratory and aorta models in places where WSS was highest. WSS is an index that cannot be obtained in vivo. In contrast, the in-vitro method based on precise numerical models can accurately calculate the changes of this parameter in the whole model. We propose that future studies model the whole respiratory system, including the upper and lower airways. Similarly, the circulatory system should be whole modeled, including the carotid arteries and the abdominal aorta. Studies using such expanded organ models will help to understand complex health conditions and diseases more precisely.

References

1. Mortazavy Beni, H., Mortazavi, H., and Islam. (2021). Biomedical and biophysical limits to mathematical modeling of pulmonary system mechanics: a scoping review on aerosol and drug delivery. Biomech Model Mechanobiol, 21, 79–87.

2. Mortazavy Beni, H., Mortazavi, H., Tashvighi, E., & Islam, M. S. (2022). Investigation of the Upper Respiratory Tract of a Male Smoker with Laryngeal Cancer by Inhaling Air Associated with Various Physical Activity Levels. Atmosphere, 13(5), 717.

3. Mortazavi, H., Mortazavy Beni, H., Aghaei, F., Sajadian, H. (2020). SARS-CoV-2 droplet deposition path and its effects on the human upperairway in the oral inhalation. Computer Methods and Programs in Biomedicine, 200(5448), 105843.

4. Mortazavy Beni, H., Mortazavi, H., Aghaei, F., Kamalipour, S. (2021). Experimental tracking and numerical mapping of novel coronavirus micro-droplet deposition through nasal inhalation in the human respiratory system. Biomech Model Mechanobiol., 20(3), 1087-1100.

5. Mortazavy Beni, H., Hassani, K., Khorramymehr, S. (2019). Study of the sneezing effects on the real human upper airway using fluid–structure interaction method. J Braz Soc Mech Sci Eng., 41(4), 181.

6. Cameron, J. R., Skofronick, J. G., and MGrant, R. (1992). Medical Physics: Physics of the body. Medical Physics Publishing Corporation.

7. Alimohammadi, M., Agu, O., Balabani, S., Díaz-Zuccarini, V. (2014). Development of a patient-specific simulation tool to analyse aortic dissections: assessment of mixed patient-specific flow and pressure boundary conditions. Med Eng Phys, 36(3), 275–84.

8. Ball, C. G., Uddin, M., Pollard, A. (2008). High resolution turbulence modelling of airflow in an idealized human extra-thoracic airway. Comput. Fluids, 37, 943–964.

9. Tse, K. M., Chang, R., Lee, H. P., Lim, S. P., Venkatesh, S. K., and Ho, P. (2013). A computational fluid dynamics study on geometrical influence of the aorta on haemodynamics. European journal of cardio-thoracic surgery: Official journal of the European Association for Cardio-thoracic Surgery, 43(4), 829–838.

10. Alaodolehei, B., Jafarian, K., Sheikhani, A., Mortazavy Beni, H. (2020). Performance Enhancement of an Achalasia Automatic Detection System Using Ensemble Empirical Mode Decomposition Denoising Method. J. Med. Biol. Eng., 40, 179–188.

11. Mortazavy Beni, H., Mortazavi, H. (2022). Mathematical modeling of the solar regenerative heat exchanger under turbulent oscillating flow: Applications of renewable and sustainable energy and artificial heart. Results Eng., 13, 100321.